Australian Journal of Basic and Applied Sciences, 7(9): 15-27, 2013
ISSN 1991-8178

Impedance Analysis as a Tool for Hydraulic Fracture Diagnostics in Unconventional Reservoirs

Amir Reza Rahmani, Mahdy Shirdel

Dept. of Petroleum & Geosystems Engineering, University of Texas at Austin, Austin, TX, USA.

Abstract: Production from unconventional reservoirs plays a key role in supplying hydrocarbon to the world's increasing energy demand. Hydraulic fracturing is one of the most advancing technologies in producing hydrocarbon from low-permeability reservoirs, especially in tight and shale formations. The geometric properties of a hydraulic fracture affect significantly the production rate from these stimulated reservoirs. Therefore, it is of utmost importance to characterize the geometric features of hydraulically-induced fractures during stimulation processes. The geometric properties of a hydraulic fracture change with fracture evolution due to stress propagation along the cracks. We have modeled such a system based on the analogy between fluidic and electric circuits. The model takes into account the dynamic alteration of hydrodynamic impedance of the fracture. The hydrodynamic impedance controls the relation between the fracture fluid flow rate and pressure drop during stimulation process. The proposed model incorporates the effects of both hydrodynamic capacitance and resistance of the fracture and the wellbore to compute the fracture impedance. Downhole measurements of pressure and flow rate can explicitly determine the hydrodynamic impedance of the fracture. Fracture impedance can also be implicitly inferred from wellhead pressure and flow rate measurements. The pulsatile nature of hydraulic fracturing treatment makes it sensible to utilize the wellhead data for the purpose of impedance monitoring based on the electromagnetic transmission line theory. We have performed extensive sensitivity analyses on the most important parameters of a single hydraulic fracture for assessing fracture impedance. These parameters include fracture thickness, fracture radial extent, and fracture shape. Through sensitivity analyses results and real-time measurement of fracture impedance, we infer the basic geometric properties of a hydraulic fracture. This research has led to an analytical approach for evaluating hydraulic fractures geometric characteristics. The approach builds an intuition toward better understanding how to design hydraulic fractures in a more efficient fashion.

Key words:

INTRODUCTION

Hydraulic fracturing is one of the most applicable topics in petroleum industry which requires further development and investigation. This process, in its most general term, encompasses injecting fluid at high rates into the well. If the pressure exceeds the tensile strength of the rock, the rock cracks open, creating a vertical plane propagating away from the wellbore. Most important geometric characteristics of the fractures include the length, height, and the width (opening). Lengths can range from hundreds to thousands of feet, height is usually hundreds of feet, and the opening is on the order of fractions of inch.

Fracture geometry determines the efficiency of a hydraulic fracture treatment and hence, is of utmost importance to production rate. In this study, our main objective is investigating and developing a tool to analyze the fracture geometry during the fracturing process based on the concept of hydraulic impedance. The notion of hydraulic impedance (for details, see Tabeling 2005) can help us characterize the complex behavior of a hydraulic fracture system more effectively through obtaining an analogous electrical system.

For this purpose we have taken the following steps in our study:

- Introducing impedance analysis for fractured wells, using the analogy between electrical circuits and hydrodynamics.
- Development of an efficient and simple tool to evaluate hydraulic fractures geometry during a typical hydraulic fracturing practice.
- Performing sensitivity analysis on fracture geometry to investigate the effect of fracture parameters on pressure and flow rate pulses.

Mainly fracture geometries are considered as rectangular or elliptical shapes. Figure 1 shows the common fracture shapes. Figure 2 shows the fracture system in conjunction to the wellbore. In our analysis we consider the coupled fracture wellbore system (Yew and Ashour, 1996).

Corresponding Author: Amir Reza Rahmani, Mahdy Shirdel, Dept. of Petroleum & Geosystems Engineering, University of Texas at Austin, Austin, TX, USA.
E-mail: arahmani@utexas.edu

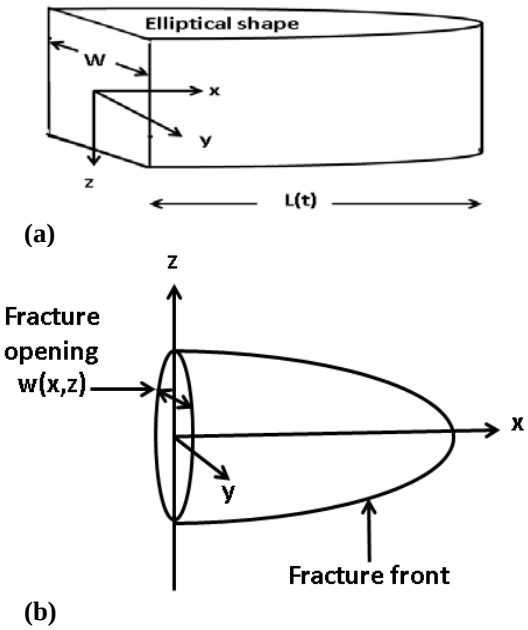

Fig. 1: Fracture geometry (a) rectangular cross section (b) elliptical cross section

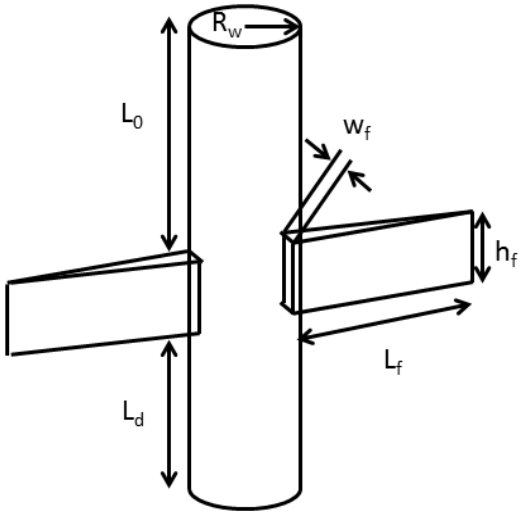

Fig. 2: Coupled wellbore/fracture system

Fluid Transient Analysis:

In microfluidics, hydrodynamic impedance is defined as the ratio of pressure (or pressure head) to the flow rate through the fluidic element as a result of the applied pressure, in the same way electric impedance is the ratio of electrical voltage to electrical current. In this section the fracture system is treated as a control volume in which instantaneous stoppage is occurred at the downstream. In fact, when the fracture is opened by increasing the fracture fluid pressure (head), the fracture growth is continued until it is stopped. These phenomena can be modeled as an instantaneous stoppage of flow stream by a valve. Figure 3 (a) shows the schematic view of the system and the control volume that momentum balance is applied. In our analysis we assume that friction and other minor losses are neglected in the wellbore. For accurate modeling of wellbore hydrodynamic, a comprehensive model (Shirdel and Sephernoori, 2011) can be used. In addition, we assume when the instant valve is closed, the fluid immediately adjacent is brought from initial velocity to rest by impulse of the higher pressure developed at the face of the valve. As soon as the first layer is brought in to rest the same action is applied to the next layer. Figure 3(b) shows the momentum equation control volume and the corresponding shock wave traveling toward upstream.

The head change at the valve, ΔH , is accompanied by a velocity change, ΔV . Writing the momentum equation in the z direction, we obtain

$$\rho A V_0^2 dt - \rho A (V_0 + \Delta V)^2 dt - \gamma \Delta H A dt = A dz \rho (V_0 + \Delta V - V_0), \quad (1)$$

Where dz can be calculated from acoustic velocity, a, and the time required for the compression shock to travel through the control volume length, Eq.2.

$$dz = (a - V_0)dt \quad (2)$$

Substituting the dz from Eq.2 into Eq.1 we have

$$\rho A V_0^2 dt - \rho A (V_0 + \Delta V)^2 dt - \gamma \Delta H A dt = A(a - V_0)dt \rho (V_0 + \Delta V - V_0) . \quad (3)$$

Rearranging the variables and assuming ΔV^2 to be small we obtain

$$\rho V_0 \Delta V - \rho a \Delta V = \gamma \Delta H \quad (4)$$

$$\Delta H = \frac{-\rho \Delta V}{\gamma}(V_0 + a) . \quad (5)$$

Eq.5 can be simplified further by assuming $\frac{V_0}{a} \ll 1$. Hence Eq.5 becomes

$$\Delta H = \frac{-\rho a \Delta V}{\gamma} = \frac{-a \Delta V}{g} = \frac{a}{gA} \Delta Q . \quad (6)$$

Eq.6 shows the relation between the head change at the valve and the velocity change. Later on, we define $\frac{a}{gA}$ as the "characteristic impedance" of the conduit. To define the acoustic velocity, we combine Eq.6 with mass balance for the given control volume in Figure 3(b).

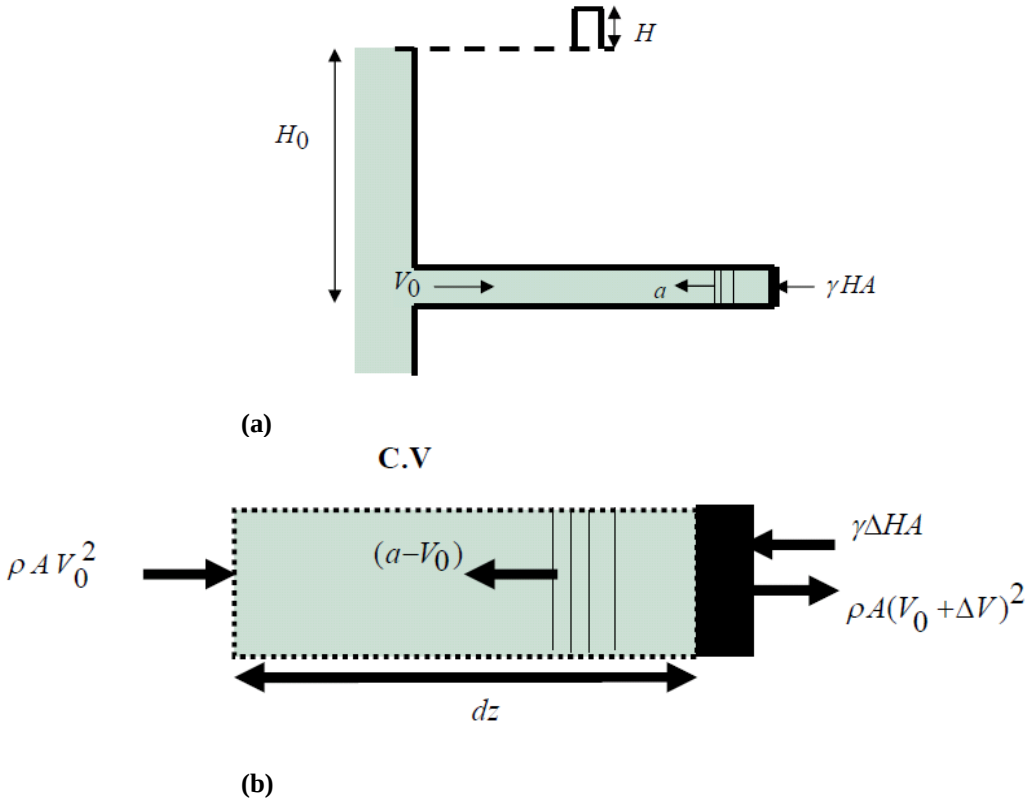

Fig. 3(a): Instant stoppage flow in horizontal fracture (b) Momentum equation applied to control volume

$$\rho A V_0 dt = \rho l.dA + \rho A.dl + Al.d\rho , \quad (7)$$

where l is dz. Assuming $dt = \frac{l}{a - V_0} \approx \frac{l}{a}$ and $dl = (V_0 + \Delta V) \times (\frac{l}{a})$, we obtain

$$-\rho A \Delta V \frac{l}{a} = \rho l.dA + Al.d\rho \tag{8}$$

$$-\frac{\Delta V}{a} = \frac{dA}{A} + \frac{d\rho}{\rho} . \tag{9}$$

Using Eq.6, we can eliminate ΔV from Eq.9.

$$a^2 = \frac{g\Delta H}{(\frac{dA}{A} + \frac{d\rho}{\rho})} . \tag{10}$$

Assuming $K = \frac{\Delta P}{(\frac{d\rho}{\rho})}$ as the bulk modulus of elasticity of the fluid, the acoustic velocity becomes:

$$a^2 = \frac{K/\rho}{1 + (\frac{K}{A})(\frac{\Delta A}{\Delta P})} . \tag{11}$$

In the following sections, Eqs.6 and 11 are frequently used for impedance calculation.

Oscillatory Flow Equations:

Fluid oscillations in systems may be analyzed by use of the linear vibration theory or electrical transmission-line theory. In this section we show the linear vibration theory to obtain the pressure head and discharge rate variations in the systems that a perturbation is induced. Using the similar momentum and mass balance equations in the Fluid Transient Analysis section, we can find the transient differential equation in a conduit (pipeline). Eqs.12 and 13 show the system of equations for a pipeline

$$(\frac{Ag}{a^2})\frac{\partial H}{\partial t} + \frac{\partial Q}{\partial z} = 0 \tag{12}$$

$$\frac{\partial H}{\partial z} + \frac{fQ^n}{2gDA^n} + \frac{1}{Ag}\frac{\partial Q}{\partial t} = 0 , \tag{13}$$

Assuming

$$\frac{\partial H}{\partial z} = H_z = \bar{H}_z + h'_z ,$$

$$\frac{\partial Q}{\partial z} = Q_z = \bar{Q}_z + q'_z ,$$

$$\frac{\partial H}{\partial t} = H_t = \bar{H}_t + h'_t ,$$

$$\frac{\partial Q}{\partial t} = Q_t = \bar{Q}_t + q'_t ,$$

$$\bar{Q}_z = \bar{H}_t = \bar{Q}_t = 0 ,$$

$$\bar{H}_z = \frac{-f\bar{Q}^n}{2gDA^n} .$$

Eqs.12 and 13 are converted to

$$Ch'_t + q'_z = 0 \tag{14}$$

$$h'_z + Lq'_t + Rq' = 0 , \tag{15}$$

where $R = \frac{32\nu}{gAD^2}$, $L = \frac{1}{gA}$, $C = \frac{gA}{a^2}$. There is an analogy between Eqs.14 and 15 and the electrical circuit equations in an RLC circuit as we will later present in impedance analysis section. Solving Eqs.14 and 15 (Wylie and Streeter, 1982), we obtain

$$q' = \frac{-Cs}{\gamma} e^{st}(C_1 e^{\gamma z} - C_2 e^{-\gamma z}) = Q(z)e^{st} \tag{16}$$

$$h' = e^{st}(C_1 e^{\gamma z} + C_2 e^{-\gamma z}) = H(z)e^{st} \ , \tag{17}$$

where C_1, C_2 are calculated from inlet pressure and disgorge pulses boundary condition:

$$C_1 = \frac{1}{2}(H_0 - Z_c Q_0) \tag{18}$$

$$C_2 = \frac{1}{2}(H_0 + Z_c Q_0) \ . \tag{19}$$

In Eqs.16 and 17, γ and s are defined as

$$\gamma = i\omega / a \tag{20}$$

$$s = \sigma + i\omega \tag{21}$$

and Z_c is defined as the characteristic impedance

$$\frac{1}{Z_c} = \frac{Cs}{\gamma} \ . \tag{22}$$

If we assume there is no friction resistivity effect, then s will only have the imaginary term as $s = i\omega$. Substituting C, s and γ in Eq.20 we obtain

$$Z_C = \frac{a}{gA} \ . \tag{23}$$

Referring to Eq.6 we arrive in

$$\frac{\Delta H}{\Delta Q} = Z_c \ . \tag{24}$$

In fact, we interpret the characteristic impedance as the ratio of head change to discharge rate change. It should be noted that this ratio is not equal to Z_c at every locations of the conduit. However, From Eqs.16 and 17, we observe that hydraulic impedance at any point is

$$Z(z) = \frac{h'}{q'} = \frac{1}{Z_c}\frac{(C_1 e^{\gamma z} + C_2 e^{-\gamma z})}{(C_1 e^{\gamma z} - C_2 e^{-\gamma z})} \tag{25}$$

In the impedance analysis section we will explain the impedance value in any location using the electrical circuit analysis approach. We observe a reasonably accurate analogy between these two methods.

Fracture and Wellbore Impedance Analysis:

Figure 4 shows the schematic of a transmission line. Figure 4.a shows a transmission line, often schematically represented as a two-wire line (Pozar, 1998). The short piece of a line of length dz in Figure 4.a can be modeled as a lumped-element circuit as shown in Figure 4.b, where *R*, *L*, G, *C* are per unit length quantities defined as follows:

R =series resistance per unit length, for both conductors in ohm/m.
L =series inductance per unit length, for both conductors, in H/m.
G =shunt conductance per unit length, in S/m.
C = shunt capacitance per unit length, in F/m.

A finite length of transmission line can be viewed as a cascade of sections of the form of Figure 4.b. From the circuit of Figure 4.b., Kirchhoff's voltage law can be applied to yield

$$v(z,t) - Rdzi(z,t) - Ldz\frac{\partial i(z,t)}{\partial t} - v(z+dz,t) = 0 \tag{26.a}$$

and Kirchhoff's current law leads to

$$i(z,t) - Gdzv(z+dz,t) - Cdz\frac{\partial v(z+dz,t)}{\partial t} - i(z+dz,t) = 0\ . \tag{26.b}$$

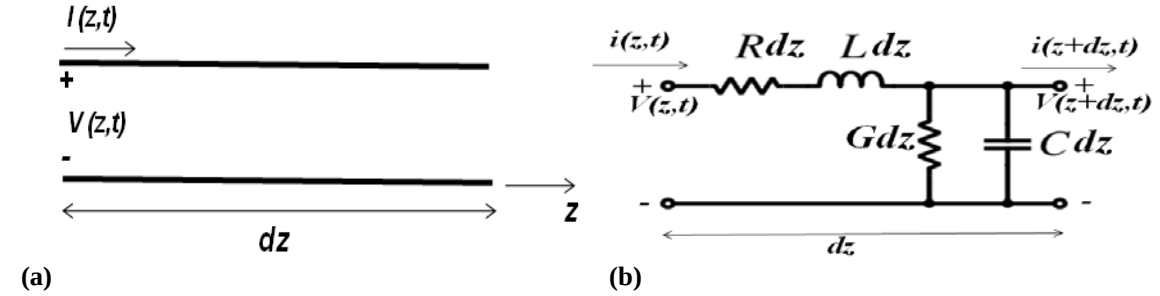

(a) **(b)**

Fig. 4: Voltage and current definitions and equivalent circuit for an incremental length of transmission line: a) Voltage and current definitions. b) Lumped-element equivalent circuit.

Dividing Eqs.26.a and 26.b by *dz* and taking the limit as *dz* goes to zero gives the following differential equations:

$$\frac{\partial v(z,t)}{\partial t} = -Ri(z,t) - L\frac{\partial i(z,t)}{\partial t} \tag{27.a}$$

$$\frac{\partial i(z,t)}{\partial z} = -Gv(z,t) - C\frac{\partial v(z,t)}{\partial t} \tag{27.b}$$

These equations are the time-domain form of the transmission line, or telegrapher equations. Note the similarity of Eqs 27.a and 27.b (setting $G = 0$) with their hydrodynamic counterparts Eqs.14 and 15. For the sinusoidal steady-state condition with cosine-based phasors, Eqs 27.a and 27.b simplify to:

$$\frac{dV(z)}{dz} = -(R+j\omega L)I(z) \tag{28.a}$$

$$\frac{dI(z)}{dz} = -(G+j\omega C)V(z) \tag{28.b}$$

The two equations can be solved simultaneously to obtain wave equations for $V(z)$ and $I(z)$:

$$\frac{d^2V(z)}{dz^2} - \gamma^2 V(z) = 0 \tag{29.a}$$

$$\frac{d^2I(z)}{dz^2} - \gamma^2 I(z) = 0 \tag{29.b}$$

where $\gamma = \alpha + j\beta = \sqrt{(R+j\omega L)(G+j\omega C)}$ is the complex propagation constant, which is a function of frequency. Traveling wave solutions to Eqs 29.a and 29.b can be found as:

$$V(z) = V_0^+ e^{-\gamma z} + V_0^- e^{+\gamma z} \tag{30.a}$$

$$I(z) = I_0^+ e^{-\gamma z} + I_0^- e^{+\gamma z} \ , \tag{30.b}$$

where the $e^{-\gamma z}$ term represents wave propagation in the +z direction, and the $e^{\gamma z}$ term represents wave propagation in the -z direction. Applying Eq.28.a to the voltage of Eq.30.a gives the current on the line:

$$I(z) = \frac{\gamma}{R + j\omega L}\left[V_0^+ e^{-\gamma z} - V_0^- e^{+\gamma z}\right] \tag{31}$$

Comparison with Eq.30.b shows that characteristic impedance, Z_c, can be defined as:

$$Z_C = \frac{R + j\omega L}{\gamma} = \sqrt{\frac{R + j\omega L}{G + j\omega C}} \tag{32}$$

to relate the voltage and current on the line as

$$\frac{V_0^+}{I_0^+} = Z_C = \frac{-V_0^-}{I_0^-} \tag{33}$$

Then Eq.30.b can be rewritten in the following form:

$$I(z) = \frac{V_0^+}{Z_C} e^{-\gamma z} - \frac{V_0^-}{Z_C} e^{\gamma z} \tag{34}$$

For a lossless transmission line (or equivalently, frictionless conduit), we can set $R = 0$ and $G = 0$:

$$\gamma = \sigma + j\beta = j\omega\sqrt{LC} \tag{35}$$

or

$$\beta = \omega\sqrt{LC} \tag{36.a}$$

$$\sigma = 0 \tag{36.b}$$

As expected for the lossless case, the attenuation constant, α is zero. The characteristic impedance of Eq.32 reduces to:

$$Z_C = \sqrt{\frac{L}{C}} \tag{37}$$

which is now a real number. The general solutions for voltage and current on a lossless transmission line can then be written as:

$$V(z) = V_0^+ e^{-j\beta z} + V_0^- e^{+j\beta z} \tag{38.a}$$

$$I(z) = \frac{V_0^+}{Z_C} e^{-j\beta z} - \frac{V_0^-}{Z_C} e^{j\beta z} \ . \tag{38.b}$$

It should be noted that the characteristic impedance does not represent any loss in the system. We have assumed that the system is frictionless. As Eq.33 suggests, this impedance relates the amplitude of the outward and inward current wave to the amplitude of the outward and inward voltage wave. In other words, no power is lost in the system due to the characteristic impedance.

The Terminated Lossless Transmission Line:

Figure 5 shows a lossless transmission line terminated in an arbitrary load impedance Z_L. This problem illustrates wave reflection on transmission lines, a fundamental problem in distributed systems. The same phenomenon occurs in our hydrodynamic system. The wellbore is acting as a transmission line and the hydraulic fractures are acting as loads as seen in Figure 5.

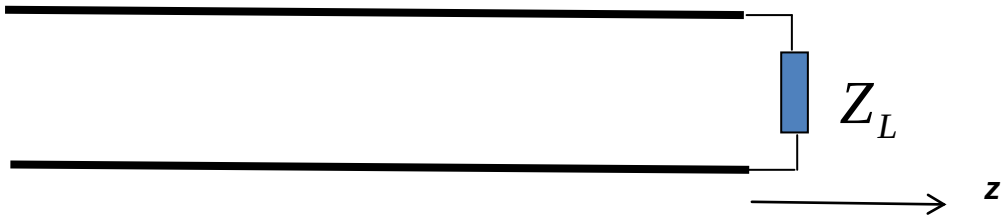

Fig. 5: Schematic of a transmission line terminated with an arbitrary load

Let's assume that a voltage wave of the form $V_0^+ e^{-jkz}$ is generated from a source at z < 0. We have already proven that the ratio of voltage to current for this source is the characteristic impedance (when there is no reflection back). However, with a load impedance at the end of a transmission line, the impedance of the system at the location of the load should be equal to the load impedance. Therefore, there should be a reflection wave excited at the load with consistent amplitude to satisfy the load (boundary) condition. Therefore, the voltage and current can be written as the sum of the incident and reflected signals as in Eqs 38.a and 38.b. The voltage and the current at the load (z = 0) are related by the load impedance:

$$Z_L = \frac{V(0)}{I(0)} = \frac{V_0^+ + V_0^-}{V_0^+ - V_0^-} Z_C \quad . \tag{39}$$

Solving for V_0^-

$$\Gamma = \frac{V_0^-}{V_0^+} = \frac{Z_L - Z_C}{Z_L + Z_C} \tag{40}$$

Therefore, the total voltage and the current are:

$$V(z) = V_0^+ \left[e^{-j\gamma z} + \Gamma e^{j\gamma z} \right] \tag{41.a}$$

$$I(z) = V_0^+ \Big/ Z_C \left[e^{-j\gamma z} - \Gamma e^{j\gamma z} \right] . \tag{41.b}$$

Therefore, the impedance at every location is:

$$Z(z) = \frac{V(z)}{I(z)} = Z_C \frac{1+\Gamma\ e^{2\gamma z}}{1-\Gamma\ e^{2\gamma z}} = Z_C \frac{1+\Gamma\ e^{2j\beta z}}{1-\Gamma\ e^{2j\beta z}} \ , \tag{42}$$

where the last equation holds when there is not any loss in the system ($R = 0$ and $G = 0$). Please note that the voltage and current on the line consist of the superposition of the incident and reflected waves (standing waves). Only when $\Gamma = 0$, there is no reflected wave. To obtain $\Gamma = 0$, the load impedance Z_L must be equal to the characteristic impedance Z_c of the transmission line, *as* seen from Eq.40. Such a load is then said to be matched to the line, since there is no reflection of the incident wave.

Especial Case: Open Circuit Boundary:

If the end of a conduit is blocked, there is no fluid flowing through the end of the conduit. This case is similar to an open circuit, *i.e.*, Z_L tending to infinity in the above transmission line analogy. For this specific case, the reflection coefficient, $\Gamma = 1$. Therefore, based on Eq.42, the impedance for such a system is:

$$Z(z) = \frac{V(z)}{I(z)} = Z_C \frac{1+e^{2j\beta z}}{1-e^{2j\beta z}} \ . \tag{43}$$

In practice, we usually have the pressure and flow rate data at the wellhead. Therefore, based on the wellhead data, we can calculate the impedance at the wellhead. Using the above analysis, one can transfer the fracture impedance to the wellhead (Holzhausen and Gooch, 1985). By comparing the wellhead data with sensitivity analysis results on fracture dimensions, we can potentially evaluate the hydraulic fracture.

Fracture Impedance Calculation:

Similar to the transmission line (here we call as wellbore), we can calculate the fracture characteristic impedance. As Eq.44 shows (Holzhausen and Gooch, 1985), the characteristic impedance of the fracture conduit is

$$Z_{cf} = \frac{a_f}{gA_f} \tag{44}$$

where A_f is the total area of the fracture where it intersects the well and a_f is the wave speed in the fracture. Assuming a penny shape fracture area for both fracture wings, we have $A_f = 2\pi bh$. Substituting A_f and Eq.11 for acoustic wave speed in Eq.44, the fracture characteristic impedance yields

$$Z_{cf} = \frac{(\frac{K/\rho}{1+(\frac{K}{A})(\frac{\Delta A}{\Delta P})})^{1/2}}{2g\pi bh} . \tag{45}$$

For the compliant conduit, we can assume that $(\frac{K}{A})(\frac{\Delta A}{\Delta P}) \gg 1$. Hence

$$Z_{cf} = (\frac{\Delta PA}{4g^2\pi^2 b^2 h^2 \rho \Delta A})^{1/2} . \tag{46}$$

Furthermore, the cross section variation, ΔA, is related to the pressure change as follows (Sneddon, 1946):

$$\Delta A = 2\Delta P h^2 (1-\nu) / \mu . \tag{47}$$

Substituting ΔA and $A = \pi bh$ in Eq.46 we obtain

$$Z_{cf} = (\frac{\mu}{8\rho g^2 \pi (1-\nu) b h^3})^{1/2} \tag{48}$$

In case the friction loss is neglected in the fracture, we can assume fracture impedance is identical to fracture characteristic impedance. Hence in our analysis we have used fracture and transmission line (wellbore) characteristic impedances to obtain the observed impedance at the wellhead.

Results:

In this section, we show the numerical results that we obtained from this study. Figures 6 and 7 illustrate the sensitivity of the fracture impedance to fracture radius (h) and fracture width (b). The plots suggest that with increasing the fracture radius and width, the fracture impedance decreases. In fact, increasing the fracture volume causes the fluid more easily to flow into the fracture. Hence, the impedance becomes smaller in larger fracture volumes. Eq.48 also justifies this behavior mathematically.

As we explained in the previous section, since data are acquired at the wellhead, the fracture impedance should be calculated at this location. Hence, we defined Eq.42 to transfer fracture impedance from bottom-hole to the wellhead. Figure 8 shows the fracture impedance transfer to the wellhead at different pressure pulse frequencies (1, 10, 100). In this graph, we have assumed that the wellbore characteristic impedance is 11250 (sec/m^2). As indicated in this figure, the fracture impedance below a certain value is transferred to a constant value and beyond that, depending on the frequency value, it declines or increases. It is also interesting that in all of the frequencies, the absolute impedances at wellhead are intersected at the fracture impedance equal to wellbore characteristic impedance.

In order to build our intuition on the hydrodynamic impedance, we have calculated the flow rate signal that we would observe at the wellhead for a given input head (pressure) signal. Figure 9 shows the input head and Figure 10 illustrates the resulting flow rate. Note the phase change in signal due to the reactive nature of our assumed hydraulic fracture (load).

One can obtain the range of fracture half-widths and fracture radii corresponding to a particular impedance value. Moreover, for a penny-shaped fracture, the fracture half-width and fracture radius are correlated through (Nolte eta al., 1981, Pollard *et al*., 1979):

$$b = \frac{2P_e h(1-\nu)}{\pi\mu} , \tag{49}$$

where P_e is the uniform internal pressure in excess of fracture closure pressure. By solving Eqs. 48 and 49 simultaneously, one can obtain the fracture half-width and fracture radius for given fracture impedance, excess pressure, and formation shear modulus. Figure 11 shows this procedure graphically. In this figure, the solid curves represent fracture radius versus fracture half-widths for fracture impedance equal to 108 s/m^2 for three different formation shear moduli. The dotted curves plot Eq. 49 for two different values of excess pressure for

formation shear modulus of 100,000 psi. The intersection of these curves with the solid curves determines the fracture half-width and radius for a given fracture impedance (based on wellhead data).

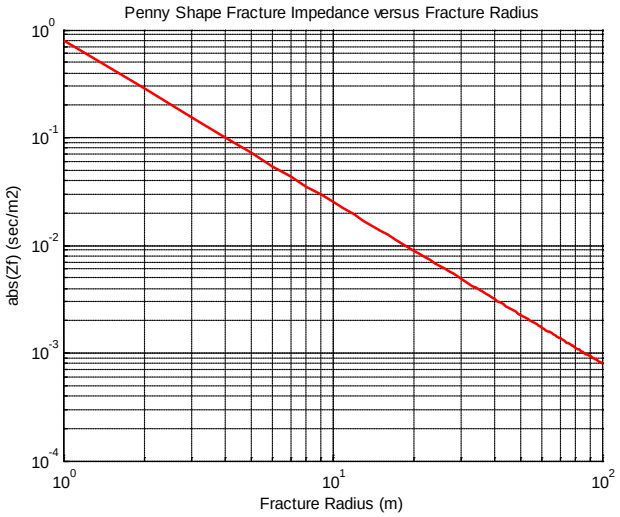

Fig. 6: Fracture impedance versus fracture radius (h)

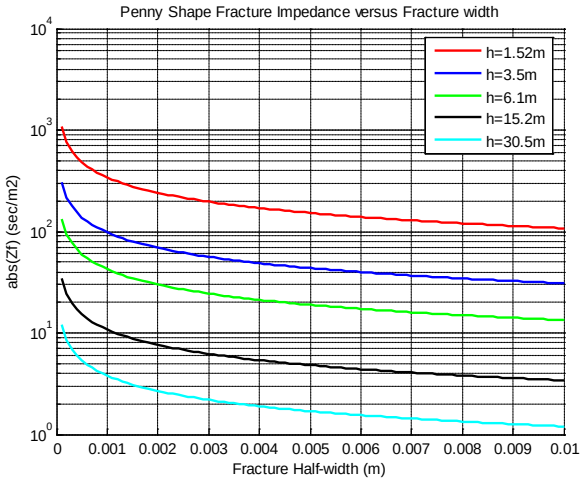

Fig. 7: Fracture impedance versus fracture half-width (b)

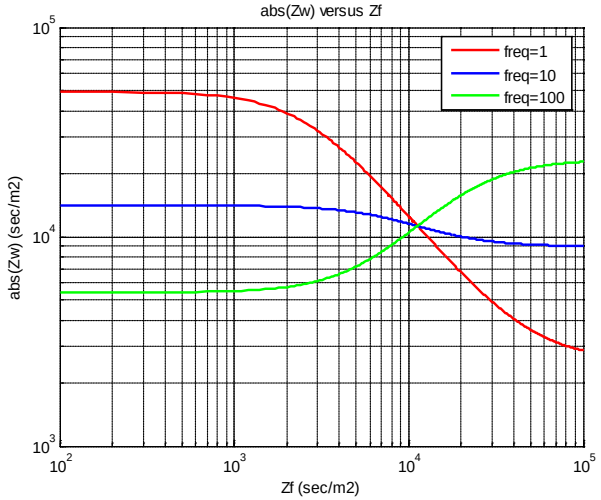

Fig. 8: Fracture impedance transfer to the wellhead fracture impedance

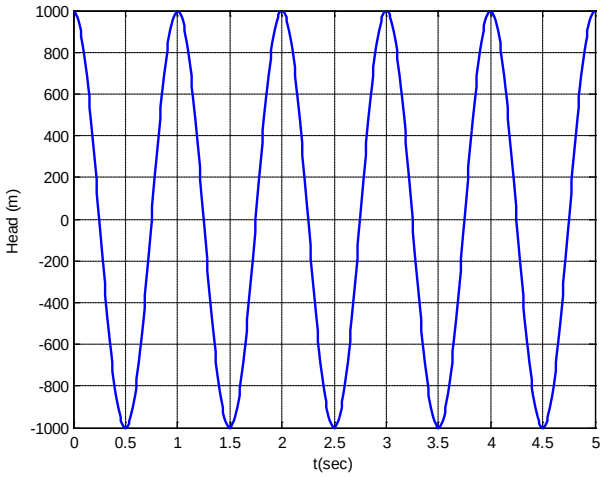

Fig. 9: Pressure (head) pulse induce in the wellhead

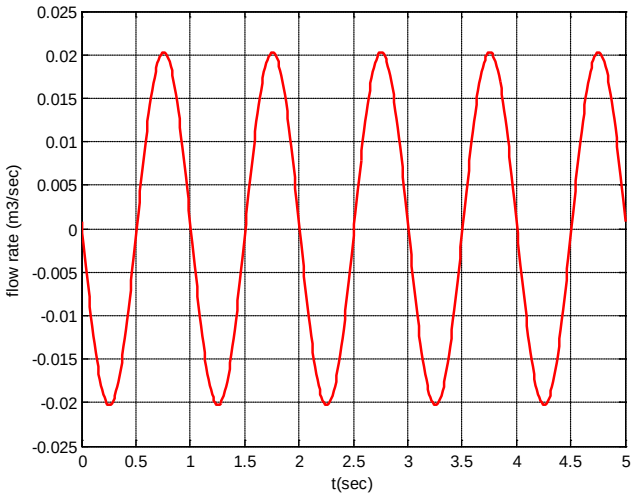

Fig. 10: The discharge rate response in the wellhead

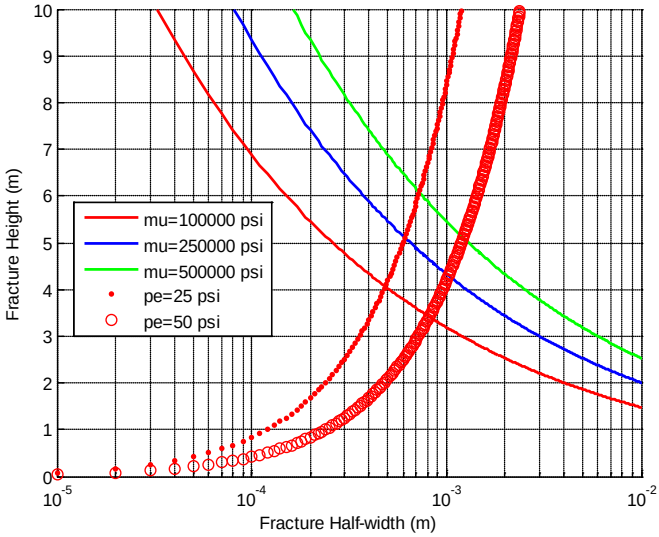

Fig. 11: Fracture geometry diagnostic using the characteristic impedance curve and fracture closure pressure constraint

Summary and Conclusions:

In this paper, we discussed fluid transient analysis in a hydraulically fractured system. We further developed an analogy between a loaded transmission line system and a hydrodynamic fractured system. We derived detailed mathematical equations using fundamental hydrodynamic equations and electrical circuit solutions. We also modified some shortcomings of the preceding studies. Utilizing the two different approaches, we derived similar formulations. Moreover, we developed the notion of impedance transfer from downhole to the wellhead and applied it for the purpose of evaluating a fractured system using wellhead pressure-flow\rate data. We finally performed sensitivity analysis for fracture geometry diagnostics to further develop an intuition on fracture geometry diagnostics using the characteristic impedance curve and fracture closure pressure constraint. Therefore, wellhead pressure/flow rate data can be used to potentially infer the fracture geometries.

Nomenclature:

w and w_f: Fracture width (m)
L and L_f: Fracture length (m)
h_f: Fracture height (m)
R_w: Wellbore radius (m)
L_d: Length along the wellbore from wellhead to fracture location (m)
ρ: Fluid density (kg/m3)
H: Maximum pressure head variation at the wellhead (m)
H_0: Static pressure head at the wellhead (m)
A: Cross-section (m^2)
A: Acoustic velocity (m/s)
V_0: Initial fluid flux (m/s)
ΔH: Pressure head variation (m)
γ: Gravity potential coefficient (ρg) (kg/m^2s^2)
z: Longitudinal coordinate (m)
dt: Time increment (s)
t: time (s)
ΔQ: Variation in flow rate (m^3/s)
ΔV: Variation in fluid flux (m/s)
g: Gravity acceleration (m/s^2)
K: Bulk modulus of elasticity (Pa)
f: Frequency (Hz)
s: Complex frequency (rad/s)
γ: Propagation constant in well (rad/s)
w: Angular frequency (rad/s)
Z_c: Characteristic impedance of well (s/m^2)
Z_f: Fracture impedance (s/m^2)
Z_w: Fracture impedance (s/m^2)
Z: Hydrodynamic impedance (s/m^2)
Γ: Reflection coefficient (unitless)
Γ_f: Downhole reflection coefficient (unitless)

REFERENCES

Dearholt, D.W. and W.R. McSpadden, 1973. "*Electromagnetic Wave Propagation*," McGraw Hill, New York.

Holzhausen, C.R. and R.P. Gooch, 1985. "Impedance of Hydraulic Fractures: Its Measurement and Use for Estimating Fracture Closure Pressure and Dimensions," SPE 13892, presented at the SPE/DOE Low permeability Gas Reservoirs held in Denver, CO. 19-22.

Shirdel, M., K. Sepehrnoori, 2011. "Development of a Transient Mechanistic Two-Phase Flow Model for Wellbores," Reservoir Simulation Symposium Conference, Woodlands, Texas, USA,

Nolte, K.G, and M.B. Smith, 1981. "Interpretation of Fracturing Pressures," J. Petr. Tech., pp: 1767-1775.

Tabeling, P., 2005. " *Introduction to Microfluidics*," Oxford University Press Inc., New York.

Pozar, D.M., 1998. "*Microwave Engineering*," John Wiley and sons, inc., New York.

Pollard, D.D. and G.R. Holzgausen, 1979. "On the Mechanical Interaction between a Fluid-filled Fracture and the Earth's Surface," Tectonophysics, 53: 27-57.

Sneddon, I.N., 1946. "The Distribution of Stress in the Neighborhood of a Crack in an Elastic Solid," Proc. Roy. Soc. A., pp: 187-229.

Wylie, E.B. and V.L. Streeter, 1982. "*Fluid Transients*," FEB Press, Ann Arbor.

Yew, C.H., A.A. Ashour, 1996. "A Study of the Fracture Impedance Method," Annual Technical Meeting of the Petroleum Society, Canada, Calgary, Alberta